Identification of faults in rotating machines using high precision FBG vibration sensor: a case study on PM schemes

Dipak Ranjan Nayak[1,3], Nilam N. Ghuge[1,2], Ambarish G. Mohapatra[3], Pramod Sharma[1], Narayan Nayak[3], Satyapriya Satapathy[3], Ashish Khanna[4]
[1]Electronics and Communication Engineering, University of Technology (UoT), Jaipur, India
[2]Electrical Engineering, JSPM's BSIOTR, Pune, India
[3]Electronics Engineering, Silicon University, Silicon Institute of Technology (SIT), Bhubaneswar, India
[4]Computer Science and Engineering, Maharaja Agrasen Institute of Technology (MAIT), Delhi, India

Article Info

Article history:

Received Jul 5, 2023
Revised Jun 15, 2024
Accepted Jun 25, 2024

Keywords:

DSS
Fault diagnosis
FBG sensor
Machine learning
Predictive maintenance
Signal processing
Vibration sensor

ABSTRACT

Predictive maintenance (PM) is a data-driven approach to performing proactive maintenance by analyzing the condition of the equipment in any industrial setting. The high-precision sensors are widely adapted to meticulously analyze critical maintenance conditions using such a data-driven approach. In a similar context, a fiber brag grating (FBG) sensor is a passive and high-precision sensor that is widely used in industries where conventional sensors are not preferred. Broadly, this article presents four sub elements of the proposed integrated system such as the design of the sensor element, signal processing scheme (SPS), machine learning (ML) model for predicting anomalies, and decision support system (DSS) to suggest maintenance actions. Also, this article highlights an experimental case study on vibration monitoring and analysis of real-time signals for making proactive maintenance decisions. An FBG vibration sensor of center wavelength 1,550 nm is designed and utilized to acquire real-time vibration signatures of a rotating machine under test. A piezoelectric vibration sensor is used with the FBG sensor to compare the vibration response obtained during the test. Pre-processing of raw signals is performed using a moving average filter (MAV) followed by a low pass filter to nullify the effect of noise. To obtain proactive maintenance decisions, a DSS model is prepared by considering the processed vibration signatures. Various maintenance conditions are tested during the experimental analysis and detailed results analysis are presented.

Corresponding Author:

Ambarish G. Mohapatra
Electronics Engineering, Silicon University, Silicon Institute of Technology (SIT)
Bhubaneswar, Odisha, India
Email: ambarish.mohapatra@gmail.com

1. INTRODUCTION

The shift in modern history from an agrarian and handicraft economy to one dominated by industry and machine production was known as the industrial revolution. Technology brought about new ways of living and working that changed society as a whole. With the introduction of mechanization, water power, and steam power, the first industrial revolution (Industry 1.0) began in the 18th century. The second industrial revolution (Industry 2.0), which began in the 19th century and centered around mass production and assembly lines employing electricity, followed. Beginning in the 1970s of the 20th century, the third industrial revolution (Industry 3.0) was characterised by the introduction of electronics, information technology systems, and automation. These developments paved the way for the fourth industrial revolution (Industry 4.0), which is associated with cyber-physical systems. Figure 1 highlights the concept of the industrial revolution from the era of the 18th Century to the 20th Century.

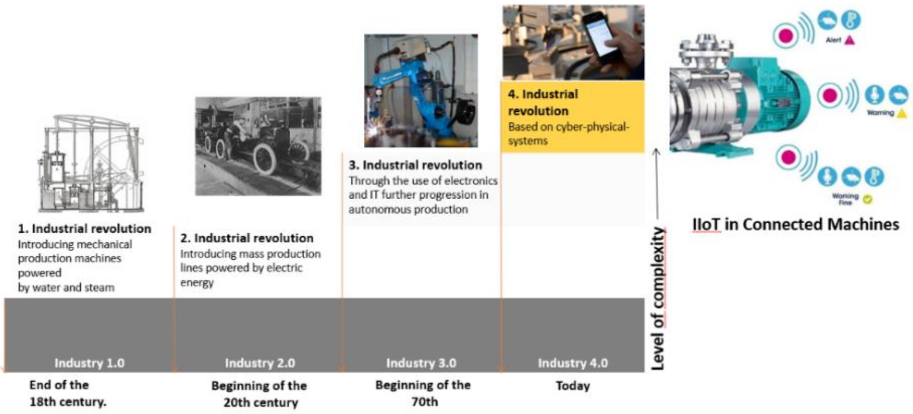

Figure 1. Industrial revolution from Industry 1.0 to Industry 4.0

Primary rotating machinery such as motors, compressors, generators, steam turbines, and high-speed engines are crucial to modern industrial processes under Industry 4.0 [1]-[3]. Precise operation and fault detection of these machines ensure stable industrial processes. Mechanical failures often manifest as vibrations [4], [5], which are key parameters for equipment health and safety evaluation [6], [7]. Therefore, measuring vibration signals for condition and fault diagnosis of rotating machinery is essential [8]. This article highlights the capability of fiber brag grating (FBG) sensors for vibration monitoring of rotating machines and interpreting the acquired vibration signature into useful machine fault diagnostics. FBG sensors are lightweight, corrosion-resistant, EMI-free, and smaller than traditional sensors. Being passive, they are suitable for dynamic distributed measurements [9], [10]. Thus, they are widely used for health monitoring and vibration measurement. Researchers have developed FBG-based vibration sensors to evaluate the performance of non-uniform FBGs under strain, temperature, and vibration loads. Chilelli *et al.* [11] explained a model of crack initiation and growth in embedded metal structures. Yao *et al.* [12] discussed FBG vibration tuning based on equal intensity beams and its optimization design.

Modeling and simulation are crucial in sensor design. Two FBGs are used to enhance vibration sensitivity: one measures strain, and the other measures vibration and temperature, as mentioned by Kouhrangiha *et al.* [13]. Torre *et al.* [14] described underwater vibration frequency. Sensor technology for vibration monitoring has become a significant research area. The broad objectives of this experimental analysis are listed below, which is shown in Figure 2.

– Design and test an FBG vibration sensor by utilizing low-cost polymers readily available
– Acquiring real-time signals from the developed FBG vibration sensor by installing it on an experimental setup consisting of a rotating motor
– Developing a signal processing scheme (SPS) for nullifying the effect of noise in the sensor signal
– Developing a machine learning (ML) model for understanding the machine anomalies of the rotating machine under laboratory test
– Developing a decision support system (DSS) scheme for generating adequate suggestions on machine maintenance operation

The signal processing and analysis are performed to understand the accurate vibration information of a motor under a vibration test. The proposed architecture of the predictive maintenance strategy with the model is described in Figure 3. This article is composed of eight sections including the introduction. The second section explains how FBG functions and how temperature affects wavelength sensitivity, including a thorough numerical analysis. SPSs are discussed in the third section, followed by statistical parameter extraction in the fourth section. The fifth section describes the proposed ML model for anomaly detection. The sixth section discusses a proposed ML model and DSS model, followed by an experimental setup, where the integration of FBG interrogator with an internet-based model is presented. The summary of the results is in section eight and is portrayed in the conclusion, followed by the reference section.

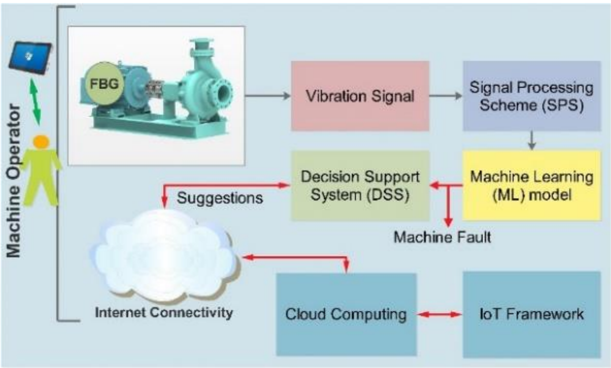

Figure 2. Proposed architecture

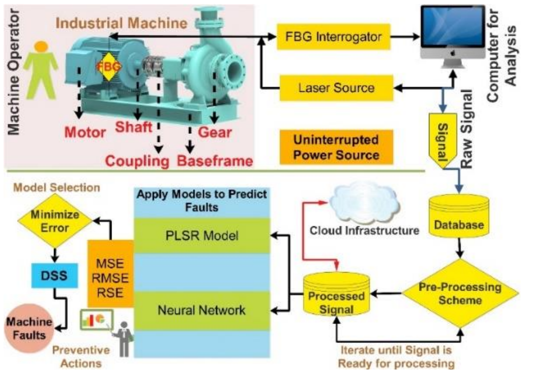

Figure 3. Proposed architecture of the predictive maintenance (PM) strategy

2. WORKING PRINCIPLE OF FIBER BRAGG GRATING

FBG technology is highly regarded for optical fiber sensors due to its simple manufacturing and strong reflected signal. The “grating” refers to the periodic change in the core’s refractive index. When light passes over the grating, some is reflected while the rest reaches the fiber’s output. The combined reflected light forms a single beam that meets the Bragg condition. When exposed to external forces like strain and temperature, the FBG changes in its grating period and Bragg refractive index. In (1) explains how the effective index of refraction of the core, N_{eff} and the grating period Λ determine the wavelength of light λ_B.

$$\lambda_B = 2 N_{eff} \Lambda \tag{1}$$

Where N_{eff} denotes the effective core refractive index, Λ is the grating period that determines the separation between two adjacent grating planes, and λ_B denotes the Bragg wavelength [15]-[18]. The principle of FBG is explained briefly and represented in Figure 4.

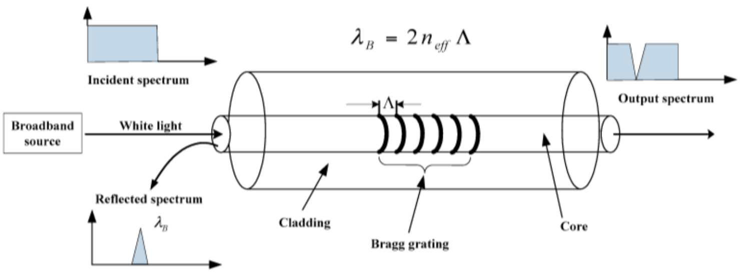

Figure 4. Basic working principle of FBG

The backward reflected peak [19], [20], whose central wavelength is defined by λ_B, forms when the Bragg condition is met. The relationship between the shift in the Bragg wavelength and the variations in the grating period ($\Delta\Lambda$) and refractive index (ΔN_{eff}), which are both strongly correlated with the original wavelength, is shown in (2).

$$\Delta\lambda_B = 2 \Delta N_{eff} \Lambda + 2 N_{eff} \Delta\Lambda \tag{2}$$

The effective change in B can be calculated using the ratio of (2) with (1).

$$\frac{\Delta\lambda B}{\lambda B} = \frac{2 \Delta \text{Neff } \Lambda + 2 \text{ Neff } \Delta\Lambda}{2 \text{ Neff } \Lambda} \tag{3}$$

$$\frac{\Delta\lambda B}{\lambda B} = \frac{\Delta \text{ Neff}}{\text{Neff}} + \frac{\Delta\Lambda}{\Lambda} \tag{4}$$

Bragg wavelength shifting ($\Delta\lambda_B$) is dependent on the FBG's temperature variation, where $\frac{\Delta\Lambda}{\Lambda} \ll \frac{\Delta \text{Neff}}{\text{Neff}}$. When considering the change in refractive index (ΔN_{eff}) with a temperature variation, the Bragg period is much smaller. Considering the reasons mentioned above, a slab-type structure was employed in the design of the FBG sensor to achieve larger fiber elongation. This resulted in a higher range of sensitivity for the sensor. In (5) and (6) can be utilized to demonstrate how temperature influences the Bragg wavelength shift ($\Delta\lambda_B$).

$$\frac{\Delta\lambda B}{\lambda B} = (1 - Pe)\Delta\varepsilon + \left[\frac{1}{\Lambda}\frac{\partial\Lambda}{\partial T} + \frac{1}{\text{Neff}}\frac{\partial \text{Neff}}{\partial T}\right]\Delta T \tag{5}$$

$$\frac{\Delta\lambda B}{\lambda B} = (1 - Pe)\Delta\varepsilon + (\alpha + \xi)\ \Delta T \tag{6}$$

The change in strain is represented by $\Delta\varepsilon$, and the strain coefficient is indicated by Pe. The temperature change is represented by ΔT, and the thermal expansion coefficient and thermo-optic coefficient of the fibre are indicated by α and ξ, respectively.

3. SIGNAL PROCESSING SCHEME

The acquired FBG signal is affected by noise due to artifacts and surrounding vibrations. This noise is mitigated by using a moving average filter (MAV). The MAV smooths time-series data by averaging N input samples. The filter's response depends on the convolution sum of the input signal $x[n]$ and the filter's impulse response, producing the output $y[n]$. This operation is expressed in (7).

$$y[n] = \frac{1}{N}\sum_{k=0}^{N-1} x[n-k] \tag{7}$$

Here, $y[n]$, $x[n-k]$ are represent the smoothed output and input signal respectvely. The filter coefficients are uniform and equal to $\frac{1}{N}$ by confirming evenly distribution across the samples. By adjustment of window size, the noise can be reduced and there is trade-off between preserving finer details in the signal and reduced noise.

4. STATISTICAL PARAMETER EXTRACTION

The signal processing methods are used to obtain statistical parameters that quantify the statistical properties of raw data. These parameters are essential for extracting meaningful information from the data. Table 1 highlights the machine faults with their categories and the statistical parameters considered to train the ML model for anomaly detection.

Table 1. Statistical parameters considered to train ML model for anomaly detection

Machine faults	Category	Statistical parameters
Loose mounting	F1	Maximum
Shaft alignment	F2	Minimum
Bent shaft	F3	Mean
Damaged bearings	F4	Median
Rotor rub	F5	Mode
Broken rotor bar	F6	Standard deviation
Stator damage	F7	Variance
Shaft imbalance	F8	Deviation from mean

5. PROPOSED MACHINE LEARNING MODEL FOR ANOMALY DETECTION

ML methods are employed in predictive maintenance for industrial machinery to enable proactive, data-driven practices. These algorithms analyze real-time and historical data from machinery to forecast probable failures and schedule maintenance tasks before breakdowns occur [21]. By using historical failure data, equipment usage, environmental factors, and other relevant information, these models predict maintenance needs with high accuracy. This approach minimizes downtime, reduces the likelihood of catastrophic failures, and optimizes maintenance costs, thereby enhancing overall equipment reliability and operational effectiveness.

6. PROPOSED MACHINE LEARNING MODEL AND DECISION SUPPORT SYSTEM

The proposed predictive maintenance scheme aims to enhance the reliability and performance of rotating machinery by combining fast fourier transform (FFT)-based frequency analysis with advanced ML models such as partial least squares regression (PLSR) and radial basis function (RBF). Leveraging an internet of thing (IoT)-based framework, the scheme enables real-time monitoring and analysis of critical frequency components associated with various fault conditions [20]-[22]. The integration of DSS further enhances the system's intelligence, providing actionable insights for maintenance personnel [23]-[26]. The PLSR model establishes a relationship between a dependent variable, 'Fault', and independent variables consisting of statistical characteristics and frequency components, maximizing covariance while considering multicollinearity [15]. For instance, a negative coefficient for 'Min' indicates a negative correlation between an increase in the minimum value and a decrease in the projected fault, while a positive coefficient for 'Mean' suggests a higher mean value is linked to a greater likelihood of the fault occurring. The intercept of 65.0530 represents the baseline fault value when all input variables are zero. The radial basis function neural network (RBFNN), with its unique three-layer configuration, uses a RBF in the hidden layer, making it effective for data processing, learning, and analysis in predictive maintenance. Initially, a gaussian distributed function determines the center and width of RBFs, followed by gradient descent for adjusting output weights. RBFNNs can approximate complex nonlinear functions, making them suitable for time-series fault prediction, accurately forecasting potential breakdowns by processing previous equipment data. This capability reduces maintenance costs, improves machinery efficiency, and minimizes downtime, despite the necessity for proper adjustment of characteristics such as number, width, center, and output weights of RBFs. Overall, the scheme effectively handles high-dimensional data and offers computational efficiency benefits.

7. EXPERIMENTAL SETUP

Machine vibration can be caused by a variety of factors, including bearings, gears, unbalance, and so on, and even small amplitudes can have a significant impact on overall machine vibration. The proposed model for the vibration measurement and analysis of a machine is shown in Figure 5. The Ibsen I-MON high-speed FBG Interrogator captures the continuously changing wavelength λ_B due to machine vibrations. Real-time signals are acquired by interfacing the FBG Interrogator with the National Instruments LabVIEW environment. Figure 6 shows the experimental setup for the proposed vibration sensing procedure. Signal processing is then used to achieve precise response data. Vibration sources have characteristic frequencies, which can be discrete or combined frequencies. Vibration measurement, a common sensing technique, detects, diagnoses, and prognoses by measuring the overall vibration level across a frequency range (10-1,000 Hz or 10-10,000 Hz). Minimal vibration machines, excluding bearing vibration, exhibit spikes in the vibration signal, indicated by the crest factor (Peak/RMS), signaling incipient failure, while high RMS levels indicate critical failure. Rolling bearings without defects generate minimal vibration, whereas defects cause high natural frequencies. Single defects, like raceway fracturing, dominate the frequency spectrum with impulsive events at raceway passing frequencies. Characteristic defect frequencies and sidebands increase with damage but eventually decrease as broadband noise and significant oscillations at shaft rotation frequency increase. Bearings at slow machine speeds produce low-energy signals that are hard to detect, and those in gearboxes are challenging to monitor due to high energy.

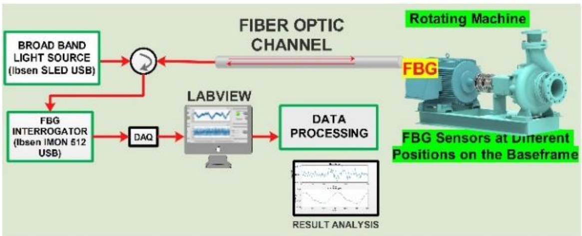

Figure 5. Proposed model for the vibration measurement and analysis of a machine

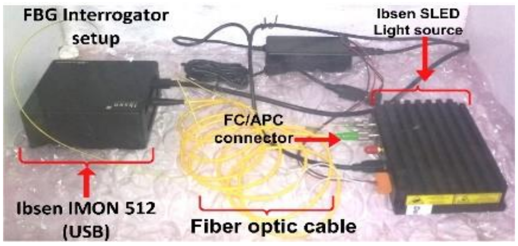

Figure 6. Experimental setup of the FBG sensor for vibration analysis

8. RESULTS ANALYSIS AND DISCUSSION

This section details the implementation of a FBG interrogator with a personal computer to acquire real-time vibration signatures under various fault conditions. Integrating the FBG interrogator with a PC enables robust data acquisition, allowing for precise monitoring and recording of vibration patterns during different fault scenarios. The raw signals recorded using an FBG sensor installed on the vibrating machine under conditions such as loose mounting (Fault: F1), broken rotor bar (Fault: F2), damaged bearing (Fault: F3), and bent shaft (Fault: F4) are shown in Figure 7. Similarly, Figure 8 displays the raw signals for shaft alignment (Fault: F5), shaft imbalance (Fault: F6), stator damage (Fault: F7), and rotor rub (Fault: F8). The application of a MAV is a key aspect of signal processing that functions to smooth out fluctuations and irregularities in the data. This proves invaluable in enhancing the accuracy and reliability of the information derived from the FBG sensor, as it effectively reduces the impact of random noise, which can often distort the true underlying signal. Figure 9 shows the smoothed signal during removal of random noise from FBG vibration signal during loose mounting condition (Fault: F1), broken rotor bar (Fault: F2), damaged bearing (Fault: F3), bent shaft (Fault: F4). Similarly, removal of random noise from FBG vibration signal during Shaft alignment (Fault: F5), shaft imbalance (Fault: F6), shaft damage (Fault: F7), and stator rub (Fault: F8) faults are briefly explained in Figure 10.

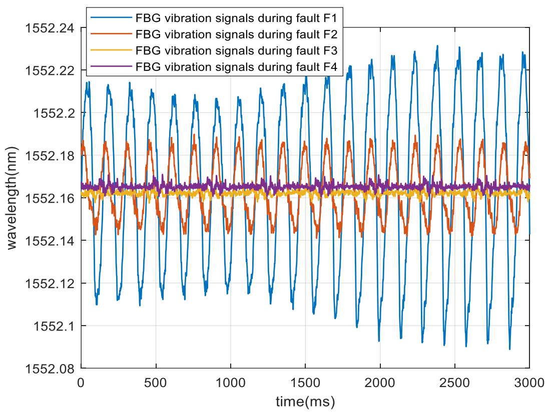

Figure 7. FBG vibration signal during loose mounting (Fault: F1), broken rotor bar (Fault: F2), damaged bearing (Fault: F3), bent shaft (Fault: F4)

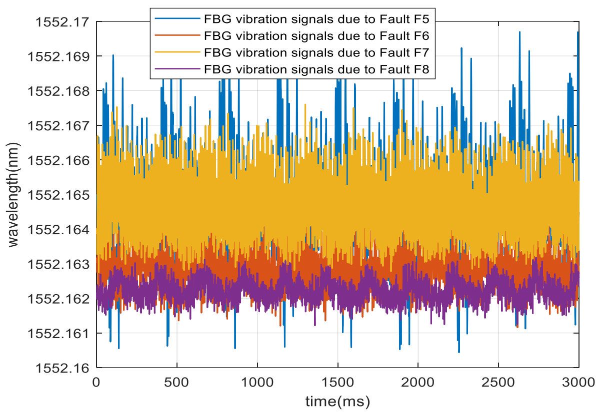

Figure 8. FBG vibration signal during shaft alignment issue (Fault: F5), shaft imbalance (Fault: F6), stator damage (Fault: F7), rotor rub (Fault: F8)

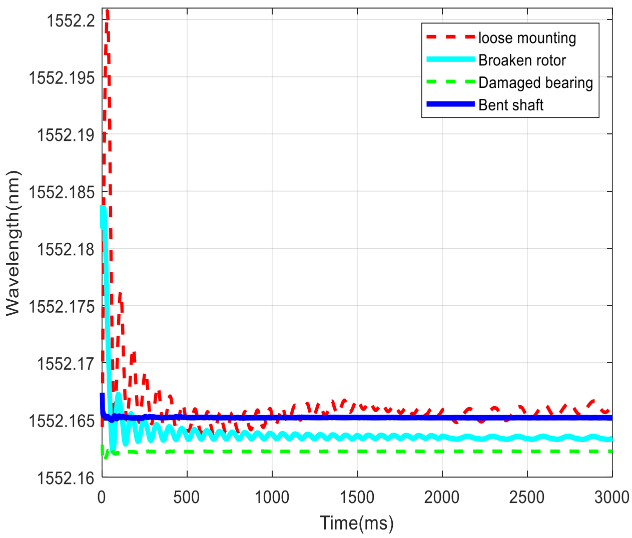

Figure 9. Removal of random noise from FBG vibration signal during loose mounting condition (Fault: F1), broken rotor bar (Fault: F2), damaged bearing (Fault: F3), and bent shaft (Fault: F4)

The FFT on the refined FBG sensor signal [27] provides insights into vibrations related to different fault conditions [28]. This approach transforms time-domain signals into frequency-domain representations, facilitating a detailed exploration of vibrational patterns linked to specific faults. It proves crucial for fault detection, condition monitoring, and structural integrity analysis [27], [28]. Similarly, FFT is used to analyze vibration signatures for various predefined faults such as loose mounting (F1), broken rotor bar (F2), damaged bearing (F3), bent shaft (F4), shaft alignment (F5), shaft imbalance (F6), shaft damage (F7), and stator rub (F8) [27], [28]. Additionally, Figure 11 illustrates the frequency response of the time domain signal during these fault conditions, showcasing the effectiveness of FFT in analyzing vibration signatures.

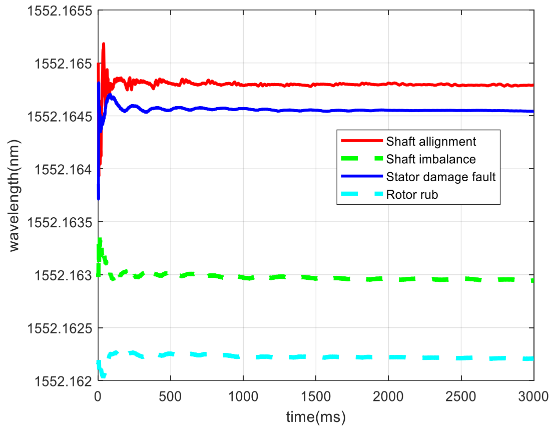

Figure 10. Removal of random noise from FBG vibration signal during shaft alignment (Fault: F5), shaft imbalance (Fault: F6), shaft damage (Fault: F7), and stator rub (Fault: F8)

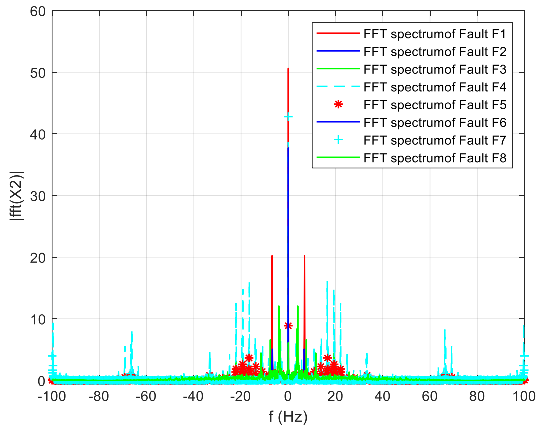

Figure 11. FFT spectrum of FBG vibration signal during different fault condition

The PLSR model is utilized to predict fault types by considering statistical parameters and frequency components [27]. PLSR effectively handles multicollinearity and establishes strong correlations between variables, aiding real-time fault identification [27]. Additionally, a radial basis type neural network is employed for fault prediction and correlation establishment like PLSR [27]. Table 2 categorizes measurements and parameters under different fault types like damaged bearings, broken rotor bars, and loose mountings, providing a comprehensive overview of the data [27].

Table 2. Statistical parameters of the pre-processed FBG vibration signal during different fault conditions

	Loose mounting	Broken rotor bar	Damaged bearing	Bent shaft	Shaft alignment	Shaft imbalance	Stator damage	Rotor rub
Faults	1	2	3	4	5	6	7	8
Min (nm)	1552.09	1552.14	1552.16	1552.161	1552.1609	1552.1612	1552.162	1552.1614
Max (nm)	1552.23	1552.19	1552.169	1552.171	1552.1693	1552.165	1552.167	1552.1634
Mean (nm)	1552.2	1552.16	1552.164	1552.166	1552.1627	1552.163	1552.1645	1552.1622
Median (nm)	1552.22	1552.21	1552.2	1552.2	1552.21	1552.21	1552.21	1552.21
Mode (nm)	1552.1	1552.201	1552.208	1552,205	1552.2207	1552.23	1552.202	1552.203
SD	0.0405	0.0139	0.0013	0.0014	0.0015	6.6965×10^{-4}	9.954×10^{-4}	3.114×10^{-4}
Variance	0.0016	0.0001927	0.756×10^{-6}	1.9911×10^{-6}	2.241×10^{-6}	4.4844×10^{-7}	9.1137×10^{-7}	9.698×10^{-8}
Mean of deviation	0.0366	0.0122	9.83×10^{-4}	0.0010	0.0012	5.4067×10^{-4}	7.82×10^{-4}	2.493×10^{-4}
F0 (Hz)	6.87	6.75	3.12	3.25	3.22	3.12	3.25	3.5
F1 (Hz)	13.62	13.65	5.62	5.67	5.62	6.5	6.7	4

Numerical parameters like amplitudes, frequencies, and statistical values are included for each fault type, creating a comprehensive dataset for fault analysis. The diverse nature of measurements and characteristics associated with different types of machinery faults is evident from the numerical values under each fault type. Figure 12 depict the comparative analysis between predicted fault types using two methodologies: PLSR and a radial basis type neural network. These figures showcase the outcomes of the research's dual approach to fault classification based on the pre-processed FBG sensor signal.

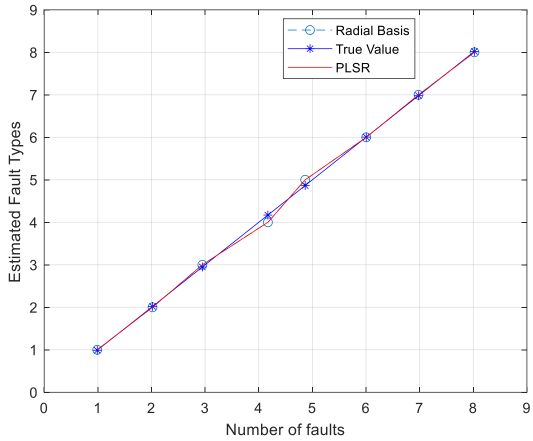

Figure 12. Estimated fault types using PLSR model and RBF neural network

Figure 12 graphically depicts the PLSR model's predictions for fault types, with each fault category represented as a distinct bar or data point on the graph. The x-axis corresponds to different fault types, while the y-axis represents predicted fault probabilities or classifications, indicating the model's confidence in predicting specific fault types. This visualization aids researchers and readers in understanding the PLSR model's performance in fault identification and differentiation among fault conditions. Analyzing the bars/data points in Figure 12 provides insights into the neural network's fault classification performance and enables a side-by-side evaluation with the PLSR model. In (7) presents the mathematical model incorporating statistical parameters and frequency components.

$$\text{Fault} = 65.0530 - (0.0084 \times \text{Min}) - (0.0898 \times \text{Max}) + (0.3218 \times \text{Mean}) - (0.2502 \times \text{Median}) - (0.0084 \times \text{Mode}) + (0.0426 \times \text{SD}) - (0.0001 \times \text{Variance}) - (0.0384 \times \text{Mean variance}) - (0.0522 \times \text{F1}) - (0.4258 \times \text{F2}) \quad (7)$$

Table 3 compares error parameters between two fault prediction models: PLSR and RBF neural network, crucial for accuracy assessment. The metrics include root mean squared error (RMSE), residual standard error (RSE), and MSE. The table highlights RBF's superior predictive accuracy over PLSR. These metrics aid researchers and practitioners in selecting the most effective model for fault prediction based on their needs and data characteristics.

Table 3. Error parameters of fault prediction models

	RMSE	RSE	MSE
PLSR	0.079966	0.998781	0.006395
RBF	0.000025	1.000000	0.000437

Table 4 outlines a DSS employing fuzzy logic to link machine faults with fault categories and suggest repair and maintenance actions [25]. This integration enhances adaptability and interpretability, addressing uncertainties in industrial applications. The article promotes proactive maintenance strategies with real-time monitoring and decision support in industrial settings.

Table 4. Input and output parameters of fuzzy logic DSS model for different fault conditions

Machine faults	Fault category	Suggestion for repair and maintenance	Suggestion type
Loose mounting	1	Tighten bolts, ensure alignment	11, 12
Shaft alignment	2	Precision alignment, regular checks	21, 22
Bent shaft	3	Replace or repair, investigate cause	31, 32
Damaged bearings	4	Prompt replacement, proactive maintenance	41, 42
Rotor rub	5	Investigate cause, ensure clearance	51, 52
Broken rotor bar	6	Motor analysis, replace bars	61, 62
Stator damage	7	Inspect and replace stator windings	71, 72
Shaft imbalance	8	Dynamic balancing, regular monitoring	81, 82

Figure 13 illustrates input and output membership functions corresponding to maintenance suggestions (Sugg1 and Sugg2) of the fuzzy DSS model, showing how fault categories (F1 to F8) are linguistically characterized within the fuzzy logic framework. Table 5 presents the fuzzy DSS rulebase, detailing logical relationships between faults and maintenance suggestions. This integration of graphical representations and a well-defined rulebase aligns with the article's objective of developing a robust fuzzy logic-based DSS for predictive maintenance as shown in Table 6, enhancing proactive maintenance decision support in industrial practices. Table 6 provides a concise overview of the testing phase for the fuzzy DSS model, connecting seamlessly with the previously discussed concepts. This table outlines specific fuzzy inputs and their corresponding fuzzy outputs, which represent the system's recommendations for proactive maintenance actions.

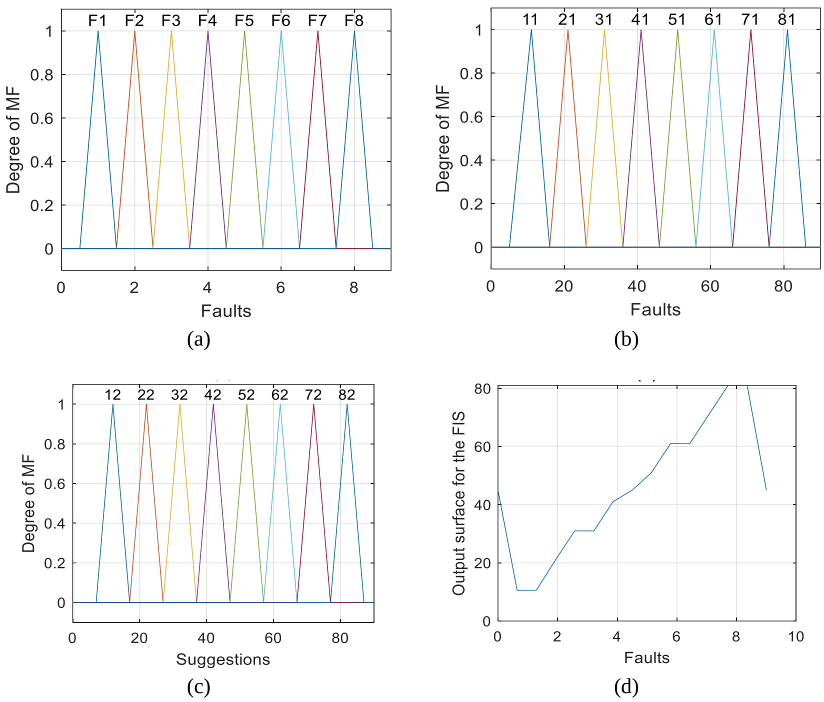

Figure 13. The input and output membership functions (MF) of the fuzzy inference system (FIS)

Table 5. Fuzzy DSS rulebase

Rule Number	Fault	Sugg1	Sugg2	Confidence
1	F1	11	12	1
2	F2	21	22	1
3	F3	31	32	1
4	F4	41	42	1
5	F5	51	52	1
6	F6	61	62	1
7	F7	71	72	1
8	F8	81	82	1

Table 6. Testing of fuzzy DSS model

Fuzzy input	Fuzzy output 1 (Suggestion 1)	Fuzzy output 2 (Suggestion 2)
2	21: Conduct precision alignment using laser alignment tools.	22: Regularly check and adjust the alignment to prevent future issues.
4	41: Replace damaged bearings promptly.	42: Implement a proactive maintenance schedule for bearing lubrication and inspection.
6	61: Perform a motor current signature analysis to identify broken rotor bars.	62: Replace the damaged rotor bars and inspect the rotor for other issues.
8	81: Use dynamic balancing techniques to correct shaft imbalance.	82: Regularly monitor and balance the rotor to prevent future issues.

9. PREDICTIVE MAINTENANCE SOLUTION ARCHITECTURE

The article extensively explores FFT-based frequency analysis [29], a well-established technique in IoT-based predictive maintenance. Frequency components corresponding to various vibration conditions are stored in a cloud-based distributed platform, facilitating prolonged monitoring and comprehensive machine health understanding over time. To address data transmission latency, a pre-processing scheme is introduced [30]. This scheme effectively mitigates latency issues, and processed information is systematically transmitted to the cloud platform at periodic intervals [31]. Figure 14 illustrates the proposed architecture integrating a DSS with the existing FBG interrogation system [32]. The architecture, designed for predictive maintenance of rotating machines using IoT, delineates technologies involved in this integrated distributed FBG sensing system, emphasizing interconnected elements for efficient and proactive machine health monitoring.

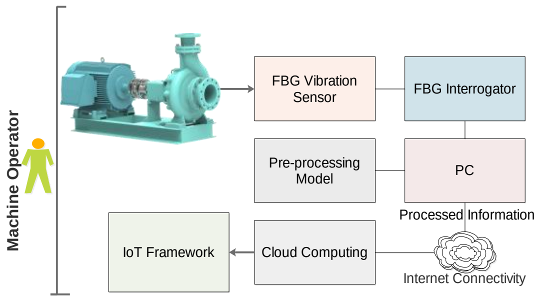

Figure 14. IoT-based solution architecture for predictive maintenance of rotating machines

The table provides insights into potential faults and their primary locations within a rotating machine [32]-[35]. One identified fault is “impeller imbalance” located in the impeller, likely caused by high vibration, indicating irregularities in weight distribution and necessitating close monitoring and corrective action. Potential faults associated with the bearing housing, such as “bearing damage” leading to a PA fan trip, can result from wear or lubrication issues, posing critical operational risks. The table also identifies potential shaft-related faults like “shaft runout” linked to high vibration or wobbling, which can significantly impact machine performance [32]-[35]. In industrial scenarios, fault identification in rotating machines using PLCs and advanced control systems, coupled with temperature and vibration data collection, enables historical performance tracking and proactive issue spotting [36]-[38]. Table 7 outlines potential failure scenarios, their primary locations, and associated causes in a rotating machine [32]-[35]. Identified faults include impeller imbalance, bearing damage, shaft damage, housing damage, and shaft runout, each with distinct causes and implications for machine reliability. This comprehensive matrix supports targeted predictive maintenance strategies, aiding in optimal machine performance and preventing severe disruptions.

Table 7. Fault identification matrix for rotating machine components

Primary location	Potential failure	Causes
Impeller	Impeller imbalance	High vibration
Bearing housing	Bearing damage	PA fan trip
	Shaft damage	
	Housing damage	
Shaft	Shaft runout	High vibration or Wobbling of the shaft

10. CONCLUSION

The study employs passive, non-contact sensors to analyze electric motor vibration, showcasing accurate fault detection. It operates effectively across diverse conditions and captures intentional faults’ vibration patterns with remarkable sensitivity. The FBG sensor-based predictive maintenance scheme integrates FFT analysis and ML, offering robust fault detection. Statistical parameters and fundamental frequency components are leveraged in constructing mathematical models using PLSR and a radial basis type neural network, providing a sophisticated approach to fault classification. Comparisons between models along with error metrics, highlight the superior predictive accuracy of the RBF model. IoT and DSS enhance real-time decision-making, aiding targeted maintenance strategies. Overall, the research advances predictive maintenance, providing a comprehensive methodology for industrial real-time monitoring and decision support.

The study's conclusion suggests significant future potential in predictive maintenance and fault detection for industrial applications. The use of passive, non-contact sensors for electric motor vibration analysis showcases a robust approach that can be further optimized and expanded across different industries. Future research can focus on enhancing fault detection algorithms, incorporating advanced signal processing techniques, and exploring new sensor technologies to improve predictive accuracy and fault classification capabilities. Additionally, the integration of IoT and DSSs offers opportunities for real-time monitoring and targeted maintenance strategies, promising advancements in industrial maintenance and reliability.

ACKNOWLEDGMENT

The authors thank the personnel of Central Glass and Ceramic Research Institute (CSIR-CGCRI), Kolkata who have provided continuous support in fabricating and calibrating the FBG sensor during this research work. The authors also thank the Silicon Institute of Technology, Bhubaneswar for providing licensed software like LabVIEW and state-of-the-art equipment like the FBG interrogator, for the successful conduction of the experiments related to this study.

REFERENCES

[1] G. Allwood, G. Wild, and S. Hinckley, "Fiber bragg grating sensors for mainstream industrial processes," *Electronics (Switzerland)*, vol. 6, no. 4, p. 92, Oct. 2017, doi: 10.3390/electronics6040092.
[2] X. Qiao, Z. Shao, W. Bao, and Q. Rong, "Fiber bragg grating sensors for the oil industry," *Sensors (Switzerland)*, vol. 17, no. 3, p. 429, Feb. 2017, doi: 10.3390/s17030429.
[3] D. R. Nayak, A. G. Mohapatra, B. Keswani, A. Mohanty, P. K. Tripathy, and A. K. Samantaray, "IoT enabled predictive maintenance of diesel generator in the context to Industry 4.0," in *Proceedings - 2021 19th OITS International Conference on Information Technology, OCIT 2021*, Dec. 2021, pp. 364–368, doi: 10.1109/OCIT53463.2021.00078.
[4] Z. Zhang, C. Liu, H. Li, Z. He, and X. Zhao, "Optical fiber grating vibration sensor for vibration monitoring of hydraulic pump," *Photonic Sensors*, vol. 7, no. 2, pp. 140–147, Jun. 2017, doi: 10.1007/s13320-017-0403-7.
[5] M. Romanssini, P. C. C. de Aguirre, L. Compassi-Severo, and A. G. Girardi, "A review on vibration monitoring techniques for predictive maintenance of rotating machinery," *Eng*, vol. 4, no. 3, pp. 1797–1817, Jun. 2023, doi: 10.3390/eng4030102.
[6] C. Du, D. Kong, and C. Xu, "Development of a fault detection instrument for fiber bragg grating sensing system on airplane," *Micromachines*, vol. 13, no. 6, p. 882, May 2022, doi: 10.3390/mi13060882.
[7] A. Mohammed and S. Djurovic, "Electric machine bearing health monitoring and ball fault detection by simultaneous thermo-mechanical fibre optic sensing," *IEEE Transactions on Energy Conversion*, vol. 36, no. 1, pp. 71–80, Mar. 2021, doi: 10.1109/TEC.2020.3003793.
[8] D. J. Meng *et al.*, "A vibration sensor based on Sagnac interferometer and fiber ring laser for fault diagnosis of bearing," *Optical Fiber Technology*, vol. 64, p. 102554, Jul. 2021, doi: 10.1016/j.yofte.2021.102554.
[9] L. Bachar, R. Klein, M. Tur, and J. Bortman, "Fault diagnosis of gear transmissions via optic fiber bragg grating strain sensors," *Mechanical Systems and Signal Processing*, vol. 169, p. 108629, Apr. 2022, doi: 10.1016/j.ymssp.2021.108629.
[10] O. Das and D. B. Das, "Smart machine fault diagnostics based on fault specified discrete wavelet transform," *Journal of the Brazilian Society of Mechanical Sciences and Engineering*, vol. 45, no. 1, p. 55, Jan. 2023, doi: 10.1007/s40430-022-03975-0.
[11] S. K. Chilelli, J. J. Schomer, and M. J. Dapino, "Detection of crack initiation and growth using fiber bragg grating sensors embedded into metal structures through ultrasonic additive manufacturing," *Sensors (Switzerland)*, vol. 19, no. 22, p. 4917, Nov. 2019, doi: 10.3390/s19224917.
[12] K. Yao *et al.*, "Design and analysis of a combined strain-vibration-temperature sensor with two fiber bragg gratings and a trapezoidal beam.," *Sensors (Switzerland)*, vol. 19, no. 16, p. 3571, Aug. 2019, doi: 10.3390/s19163571.
[13] F. Kouhrangiha, M. Kahrizi, and K. Khorasani, "Structural health monitoring: modeling of simultaneous effects of strain, temperature, and vibration on the structure using a single apodized π-Phase shifted FBG sensor," *Results in Optics*, vol. 9, p. 100323, Dec. 2022, doi: 10.1016/j.rio.2022.100323.
[14] O. de la Torre, I. Floris, S. Sales, and X. Escaler, "Fiber bragg grating sensors for underwater vibration measurement: potential hydropower applications," *Sensors*, vol. 21, no. 13, p. 4272, Jun. 2021, doi: 10.3390/s21134272.
[15] N. Nayak, B. Keswani, D. R. Nayak, P. Sharma, A. G. Mohapatra, and A. Khanna, "Fiber Bragg grating temperature sensor and calibration scheme in high magnetic field environment: An application for aluminium electrolysis cell in potline," in *3rd IEEE 2022 International Conference on Computing, Communication, and Intelligent Systems, ICCCIS 2022*, Nov. 2022, pp. 86–90, doi: 10.1109/ICCCIS56430.2022.10037719.
[16] A. G. Mohapatra *et al.*, "Fiber Bragg grating sensors driven structural health monitoring by using multimedia-enabled iot and big data technology," *Multimedia Tools and Applications*, 2022, doi: 10.1007/s11042-021-11565-w.
[17] R. Li, Y. Chen, Y. Tan, Z. Zhou, T. Li, and J. Mao, "Sensitivity enhancement of FBG-based strain sensor," *Sensors (Switzerland)*, vol. 18, no. 5, p. 1607, May 2018, doi: 10.3390/s18051607.
[18] A. G. Mohapatra, P. K. Tripathy, M. Mohanty, and A. Khanna, "IoT enabled distributed cardiac monitoring using fiber bragg grating (FBG) sensing technology," *SSRN Electronic Journal*, 2021, doi: 10.2139/ssrn.3842806.
[19] A. A. Suryandi, N. Sarma, A. Mohammed, V. Peesapati, and S. Djurović, "Fiber optic fiber bragg grating sensing for monitoring and testing of electric machinery: current state of the art and outlook," *Machines*, vol. 10, no. 11, p. 1103, Nov. 2022, doi: 10.3390/machines10111103.
[20] Z. (Family) Glasser, N. Simor, A. S. Kalnitsky, E. Liokumovitch, S. Bank, and S. Sternklar, "Enhancing the performance of FBG sensors with a wide-band interrogation system," *SSRN Electronic Journal*, 2022, doi: 10.2139/ssrn.4061392.
[21] A. A. A. Shabaneh and R. S. M. Daraghma, "Design a remote sensing of multi-BOTDR fiber optic sensors for fuel pipeline monitoring," *Telkomnika (Telecommunication Computing Electronics and Control)*, vol. 21, no. 1, pp. 60–69, Feb. 2023, doi: 10.12928/TELKOMNIKA.v21i1.24255.
[22] M. I. R. Radzman *et al.*, "Pipe leakage detection system with artificial neural network," *IAES International Journal of Artificial Intelligence (IJ-AI)*, vol. 11, no. 3, p. 977, Sep. 2022, doi: 10.11591/ijai.v11.i3.pp977-985.

[23] S. Suhadi, M. Nur, S. Sulistyowati, and A. Suroso, “Matic motorcycle transmission damage detection system using internet of things-based expert system,” *Indonesian Journal of Electrical Engineering and Computer Science (IJEECS)*, vol. 26, no. 2, p. 1018, May 2022, doi: 10.11591/ijeecs.v26.i2.pp1018-1026.
[24] A. G. Mohapatra and S. K. Lenka, “Neuro-fuzzy-based smart DSS for crop specific irrigation control and SMS notification generation for precision agriculture,” *International Journal of Convergence Computing*, vol. 2, no. 1, p. 3, 2016, doi: 10.1504/ijconvc.2016.080394.
[25] A. Hamas, A. Muneer, and S. M. Fati, “Smart security door system using SMS based energy harvest,” *International Journal of Electrical and Computer Engineering (IJECE)*, vol. 11, no. 4, pp. 3410–3423, Aug. 2021, doi: 10.11591/ijece.v11i4.pp3410-3423.
[26] Suherman, Fahmi, U. Hasnita, and Z. Herri, “Design and characteristics assessment of wireless vibration sensor for buildings and houses,” *Indonesian Journal of Electrical Engineering and Computer Science (IJEECS)*, vol. 21, no. 3, pp. 1381–1388, 2021, doi: 10.11591/ijeecs.v21.i3.pp1381-1388.
[27] M. A. Lilo and M. J. Mahammad, “Design and implementation of wireless system for vibration fault detection using fuzzy logic,” *IAES International Journal of Artificial Intelligence*, vol. 9, no. 3, pp. 545–552, 2020, doi: 10.11591/ijai.v9.i3.pp545-552.
[28] A. Sitorus, Novrinaldi, and R. Bulan, “Non-invasive moisture content measurement system based on the ESP8266 microcontroller,” *Bulletin of Electrical Engineering and Informatics (BEEI)*, vol. 9, no. 3, pp. 924–932, 2020, doi: 10.11591/eei.v9i3.2178.
[29] K. Sodha, F. S. George, K. Vijayakumar, and D. Sattianadan, “A novel collective health monitoring of a wind park,” *Indonesian Journal of Electrical Engineering and Computer Science (IJEECS)*, vol. 21, no. 2, pp. 625–634, 2020, doi: 10.11591/ijeecs.v21.i2.pp625-634.
[30] G. A. Mutiara, N. Suryana, and O. Mohd, “WSN nodes power consumption using multihop routing protocol for illegal cutting forest,” *Telkomnika (Telecommunication Computing Electronics and Control)*, vol. 18, no. 3, pp. 1529–1537, 2020, doi: 10.12928/TELKOMNIKA.v18i3.14844.
[31] V. K. Quy, N. V. Hau, D. V. Anh, and L. A. Ngoc, "Smart healthcare IoT applications based on fog computing: architecture, applications and challenges," *Complex Intelligent Systems,* vol. 8, pp. 3805–3815, 2022. DOI: 10.1007/s40747-021-00582-9.
[32] F. S. Ahmed and N. A. A. B. Al-Jawady, “Control of prosthetic hand by using mechanomyography signals based on support-vector machine classifier,” *Indonesian Journal of Electrical Engineering and Computer Science (IJEECS)*, vol. 23, no. 2, pp. 1180–1187, 2021, doi: 10.11591/ijeecs.v23.i2.pp1180-1187.
[33] Edidas and R. R. Putra, “Designing and building earthquake warning system with Arduino and web-based SES60 SLP sensor,” *Bulletin of Electrical Engineering and Informatics (BEEI)*, vol. 11, no. 1, pp. 581–588, 2022, doi: 10.11591/eei.v11i1.3546.
[34] G. Mustafa and S. Khushnood, “Early faults diagnosis and severity assessment of rolling element bearings on wireless signal transfer,” *Bulletin of Electrical Engineering and Informatics (BEEI)*, vol. 11, no. 1, pp. 221–230, 2022, doi: 10.11591/eei.v11i1.3548.
[35] G. Dinardo, L. Fabbiano, and G. Vacca, “A smart and intuitive machine condition monitoring in the Industry 4.0 scenario,” *Measurement: Journal of the International Measurement Confederation*, vol. 126, pp. 1–12, 2018, doi: 10.1016/j.measurement.2018.05.041.
[36] A. Mutharasan and P. Chandrasekar, “Fault detection and power quality analysis of wind turbine system using integrated systems,” *International Journal of Power Electronics and Drive Systems*, vol. 13, no. 1, pp. 576–585, 2022, doi: 10.11591/ijpeds.v13.i1.pp576-585.
[37] I. H. A. Al-Had, F. M. Mohammed, and J. A. K. Mohammed, “Modeling and simulation of electro-hydraulic telescopic elevator system controlled by programmable logic controller,” *Indonesian Journal of Electrical Engineering and Computer Science (IJEECS)*, vol. 27, no. 1, pp. 71–78, 2022, doi: 10.11591/ijeecs.v27.i1.pp71-78.
[38] O. F. Al-Hardanee, İ. Çankaya, A. A. Muhsen, and H. Canbolat, “Design a control system for observing vibration and temperature of turbines,” *Indonesian Journal of Electrical Engineering and Computer Science (IJEECS)*, vol. 24, no. 3, pp. 1437–1444, 2021, doi: 10.11591/ijeecs.v24.i3.pp1437-1444.

BIOGRAPHIES OF AUTHORS

Dipak Ranjan Nayak is a research scholar at UOT, Jaipur, and an Assistant Professor in the Department of Electrical and Electronic Engineering at Silicon University, Bhubaneswar, Odisha, India. His research focuses on optical sensors, control systems, and ML for IoT, with several published papers in reputable journals and conferences. He can be contacted at email: deepak.ranjan@silicon.ac.in.

Nilam N. Ghuge received his BE in Instrumentation from North Maharashtra University in 1996, ME in Instrumentation with a specialization in Computerized Process Control from SRTM University Nanded in 2007, and Ph.D. in Electronics and Communication Engineering from JJT University in 2017. Currently, he is a Professor and Head of Electrical Engineering at JSPM’s Bhivarabai Sawant Institute of Technology and Research, Pune. His research interests include image processing, signal processing, control systems, sensors, and networks. He received a university grant for developing a Control and PLC Lab and is an expert evaluation committee member for NEAT 3.0 products/courses by AICTE, New Delhi. He is also a Member of the Board of Studies in Electrical Engineering at Solapur University. He can be contacted at email: ghuge1974@gmail.com.

Ambarish G. Mohapatra is working as an Associate Professor in the Department of Electronics Engineering at Silicon University, Bhubaneswar, Odisha, India. His current research interests include optical sensors, wireless sensor networks, AI, ML IoTs. Prof. (Dr.) Mohapatra has published 14 SCI Papers, 20 SCOPUS papers, 20 chapters, 25 Papers in National and International conferences. He has also published 3 books with a national and international publisher and many times members of SCI, Scopus indexed international conference/symposium. He can be contacted at email: ambarish.mohapatra@gmail.com.

Pramod Sharma holds the position of a Professor at the University of Technology located in Jaipur, Rajasthan, India. Within the realm of academia, his primary research pursuits revolve around cutting-edge technologies such as IoT, wireless sensor networks, artificial intelligence, and ML. As an accomplished researcher, Prof. (Dr.) Pramod Sharma has contributed significantly to the scholarly community by publishing numerous papers in reputable journals and conferences, thereby enriching the collective knowledge base in his areas of expertise. He can be contacted at email: pramod.sharma@deepshikha.org.

Narayan Nayak holds the position of Associate Professor in the Department of Electronic and Instrumentation Engineering at Silicon University, located in Bhubaneswar, Odisha, India. His professional focus extends across various cutting-edge domains, including optical sensors, control systems, signal processing, AI, ML, and the IoT. Engaged in advancing knowledge within these fields, Prof. Narayan Nayak has made significant contributions to the academic community, as evident from his substantial publication record. Numerous papers authored by him have been featured in reputable journals and conferences, reflecting his dedication to the ongoing discourse and innovation in his areas of expertise. He can be contacted at email: nnayak08@gmail.com.

Satyapriya Satapathy is pursuing a Ph.D. in Electronics Engineering at Silicon University, Bhubaneswar, Odisha, India. His professional focus includes optical sensors, control systems, signal processing, AI, ML, and IoT. Er. Satapathy has significantly contributed to these fields, with numerous papers published in reputable journals and conferences. He is also holding the position of Senior Assitant Professor at Biju Patnaik National Steel Institute (BPNSI), Jajpur, Odisha, India. He can be contacted at email: satyapriya.satapathy@gmail.com.

Ashish Khanna currently serves as an Associate Professor at the Maharaja Agrasen Institute of Technology in Delhi, India. His research focus encompasses areas such as IoT, wireless sensor networks, AI, and ML. Additionally, he has authored numerous edited books in collaboration with both national and international publishers. Moreover, Prof. (Dr.) Ashish Khanna has been a frequent participant in conferences and symposiums indexed in SCI and Scopus, contributing to the academic discourse on a global scale. He can be contacted at email: ashishkhanna@mait.ac.in.